

STMDNet: A Lightweight Directional Framework for Motion Pattern Recognition of Tiny Target

Mingshuo Xu[†], Hao Luan[†], Zhou Daniel Hao, Jigen Peng, and Shigang Yue^{*}, Senior Member, IEEE

Abstract—Recognizing motions of tiny targets—only few dozen pixels—in cluttered backgrounds remains a fundamental challenge when standard feature-based or deep learning methods fail under scarce visual cues. We propose STMDNet, a model-based computational framework to Recognize motions of tiny targets at variable velocities under low-sampling frequency scenarios. STMDNet designs a novel dual-dynamics-and-correlation mechanism, harnessing ipsilateral excitation to integrate target cues and leakage-enhancing-type contralateral inhibition to suppress large-object and background motion interference. Moreover, we develop the first collaborative directional encoding-decoding strategy that determines the motion direction from only one correlation per spatial location, cutting computational costs to one-eighth of prior methods. Further, simply substituting the backbone of a strong STMD model with STMDNet raises AUC by 24%, yielding an enhanced STMDNet-F. Evaluations on real-world low-sampling frequency datasets show state-of-the-art results, surpassing the deep learning baseline. Across diverse speeds, STMDNet-F improves mF₁ by 19%, 16%, and 8% at 240Hz, 120Hz, and 60Hz, respectively, while STMDNet achieves 87 FPS on a single CPU thread. These advances highlight STMDNet as a next-generation backbone for tiny target motion pattern recognition and underscore its broader potential to revitalize model-based visual approaches in motion detection. Code is available at <https://github.com/MingshuoXu/STMDNet>.

Index Terms—Tiny target motion recognition, Visual motion detector, Dual dynamic and correlate, Collaborative directional encoding-decoding, Variable velocities, Low sampling frequencies.

I. INTRODUCTION

MOTION detection is a fundamental capability of visual systems, enabling intelligent agents to perceive their surroundings, track moving objects, and make autonomous decisions in complex environments. Among these tasks, recognizing the motion of tiny targets is particularly crucial because it allows for the early identification of potential objects that occupy only **few degrees or a dozen pixels**¹ in the visual field and lack distinct features such as contour, shape, or color, due

Mingshuo Xu, Zhou Daniel Hao, and Shigang Yue are with the School of Mathematics and Computing Science, University of Leicester, Leicester LE1 7RH, UK. E-mail: {mx60, d.hao, sy237}@leicester.ac.uk.

Hao Luan is with the Tianjin Key Laboratory of Information Sensing and Intelligent Control, School of Automation and Electrical Engineering, Tianjin University of Technology and Education, Tianjin 300222, China. E-mail: hao.luan@hotmail.com.

Jigen Peng is with the Machine Life and Intelligence Research Center, Guangzhou University, Guangzhou 510006, China. E-mail: jg-peng@gzhu.edu.cn.

[†]Mingshuo Xu and Hao Luan contributed equally to this work.

^{*}Corresponding author: Shigang Yue.

¹Less than 100 pixels or 1% of the total pixels in an image, sometimes named small target in some work.

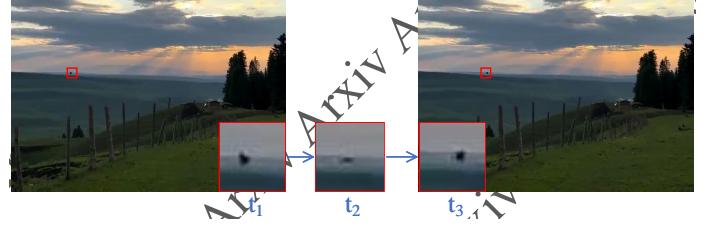


Fig. 1. Demonstration of a small / tiny moving target (a flying bird) in the cluttered moving background across three time frames t_1 , t_2 , and t_3 , with the bird highlighted and zoomed-in in red boxes for better visibility. The bird, occupying only few dozen pixels, presents a challenging detection task due to its variable outline caused by flapping wings and its minimal size within the scene.

to their distance from the observer. A flying bird, an example, is shown in Fig. 1.

Traditional motion detection methods can be mainly categorized as feature-based and motion-based. Feature-based methods typically associate results from image detectors or match image features across adjacent frames to recognize motion, making them unsuitable for featureless tiny targets [1]. In addition, motion-based techniques include optical flow [2], background subtraction [3], and other classical computer vision methods like random projection [4]. Yet these methods prioritize prominent object motion and often disregard tiny target motion as noises.

Thus, some research has shifted toward developing new mechanisms prioritizing motion detection for tiny targets. A notable example is the small target motion detector (STMD), inspired by the physiological neurons found in insect visual systems that respond intensely to targets covering only 1-3 degrees of their visual field [5]–[8]. In [1], STMDs have demonstrated superior performance compared to state-of-the-art (SOTA) deep learning models. Plus, the extremely fast processing speed makes it stand out in real-time systems.

The STMD models incorporate a delay-and-correlate mechanism, derived from the elementary motion detector (EMD) [9]–[11], as shown in Fig. 2 (A) and (B). This mechanism is a foundational concept for understanding how physiological visual systems detect motion through compact and efficient networks, particularly in low-level pathways [12]. However, despite its widespread use and historical significance, the mechanism performs optimally only when its delay parameter precisely matches the object’s length-to-velocity ratio based on the relationship between distance, speed, and time. Consequently, it is challenging to set an optimal parameter to detect tiny targets with widely varying velocities and sizes in real-world scenarios, thereby limiting STMD

performance. Moreover, the existing STMD models struggle to capture tiny moving targets at low sampling frequencies (less than 200 Hz) due to the under-utilization of temporal cues, further reducing their applicability in real-time systems [1].

To overcome the limitations of traditional delay-and-correlate approaches, we propose a novel lightweight directional framework, STMDNet. This framework comprises a new dual-dynamics-and-correlation mechanism and the first collaborative directional encoding-decoding strategy, demonstrating superior performances in locating and orientating, respectively, under low sampling frequencies.

The dual-dynamics-and-correlation mechanism utilizes a leaky current membrane equation to calculate dynamic potentials in ON-OFF channels, where an ipsilateral excitation and contralateral inhibition structure define their connectivity, as shown in Fig. 2 (C). Specifically, ipsilateral excitation captures tiny-target motion cues, while leakage-enhancing-type contralateral inhibition filters out false alarms from large-object and background motion. Next, these two potentials, dual dynamics, are correlated to locate motion, overcoming limitations in traditional EMD mechanisms related to the object’s length-to-velocity ratio, demonstrated in Fig. 5 (D).

The collaborative directional encoding-decoding strategy is the first to implement shared encoding combined with spatially-integrated decoding. It applies indicated division between the same spatial dual dynamics to get the shared encoding, improving accuracy, robustness, and efficiency compared to the delay-and-correlate mechanism (see Fig. 3). Accuracy improves due to focusing on motion cues between edges, which inherently reduces interference from irrelevant background motion and thus enhances robustness. Efficiency occurs by spatially integrated decoding with shared encoding, using only a single correlation at each spatial location rather than the eight required by the isolated directional encoding-decoding strategy integrated with the delay-and-correlation mechanism.

Then, sharing dual dynamics for locating and orientating forms a lightweight yet efficient directional backbone STMDNet based on the four-layer structure found in the insect brain (Fig. 4 (A) and (B)). To confirm its compatibility as a backbone, we extend it with a feedback pathway proposed in [13], resulting in an improved version of STMDNet-F, as shown in Fig. 4 (C).

Next, we demonstrate STMDNet’s effectiveness in recognizing tiny target motion patterns across a wide velocity range and low sampling frequency scenarios, surpassing the traditional delay-and-correlate method in both locating and orientating. Further, with STMDNet as its backbone, STMDNet-F demonstrates a significant improvement of 24% over its original version, a strong STMD baseline developed in [13]. Evaluation on real-world datasets, STMDNet-F significantly improves 8%, 16%, and 19% F_1 score at 60 Hz, 120Hz, and 240 Hz, respectively, compared to SOTA models, including the deep-learning method, listed in Tab. II. In addition, STMDNet achieves approximately 87 FPS in a signal CPU thread, reaching the highest speed among directional models.

In conclusion, STMDNet improves locating performance across a broad velocity spectrum, optimizes direction determi-

nation, and enhances low sampling frequency implementation, providing potential insight into model-based / knowledge-based methods. The innovations of this paper are fourfold:

- **Dual-dynamics-and-correlate mechanism:** We propose a novel mechanism capturing motion cues across multiple velocities, removing the tight coupling to the fixed size-to-velocity ratio inherent in the traditional delay-and-correlate approach. This mechanism enhances the locating performance while facilitating orientating and low sampling frequency implementation.
- **Collaborative directional encoding-decoding strategy:** We develop the first strategy that adopts a globally shared encoding and spatially integrated decoding to achieve the local direction, reducing the computational load to one-eighth of that required by the current strategy. It also improves robustness by mitigating interference from background motion and enhances accuracy by focusing on current motion edges.
- **Superior directional backbone STMDNet:** STMDNet achieves the fastest speed among directional models by effectively utilizing dual dynamics for locating and orienting, achieving approximately 87 FPS operations on a single thread within a CPU. In addition to its lightweight advantage, we have systematically verified its effectiveness in locating, orienting, and low-sampling-frequency applications.
- **Revitalizing STMD as the new SOTA:** We introduce STMDNet-F by substituting STMDNet as the backbone for a strong baseline, resulting in an improvement of about 24%. Evaluations in the real dataset RIST demonstrate that STMDNet-F outperforms SOTA models, including the deep learning method, improving up to 19%, 16%, and 8% at 240Hz, 120Hz, and 60Hz, respectively.

The rest of this paper is organized as follows. Firstly, Sect. II reviews the related studies, including delay-and-correlate mechanisms and small target motion detectors. Then, Sect. III presents the proposed dual-dynamics-and-correlate mechanism and collaborative directional encoding-decoding strategy, followed by a detailed description of the STMDNet and its enhanced version, STMDNet-F. Next, Sect. IV reports the experimental results, including systematic evaluations of effectiveness and comparisons in the real-world dataset. Finally, some conclusions are given in the last Sect. V.

II. RELATED WORK

In this section, we first review the delay-and-correlate mechanisms and their application in motion detection. Next, we introduce STMDs with detailed descriptions of two backbones, ESTMD and DSTMD.

A. Delay-and-correlate mechanisms

The delay-and-correlate mechanism is derived from the elementary motion detector (EMD). Here we review EMD and motion detectors based on this mechanism.

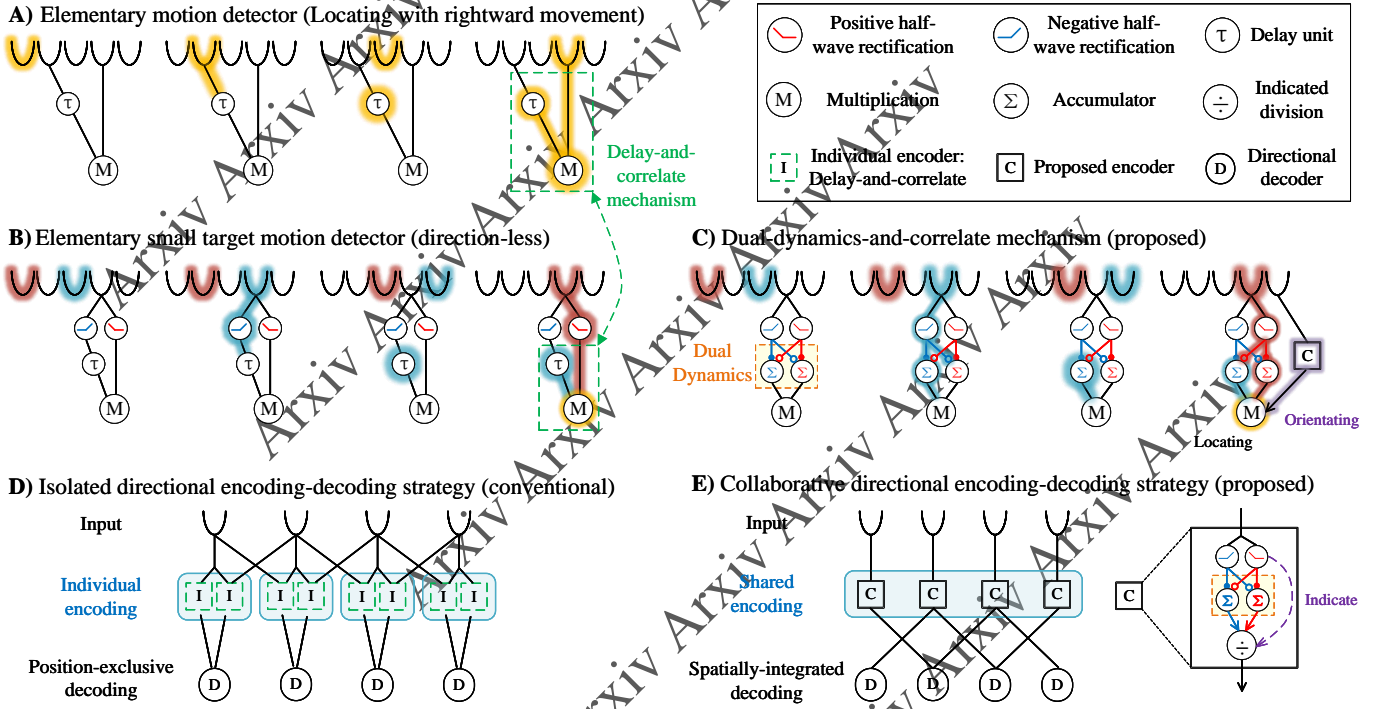


Fig. 2. Comparison of conventional and proposed mechanisms and strategies for target localization and orientation. Panel (A) depicts the prototype of the delay-and-correlate mechanism, the Elementary Motion Detector (EMD) [9], which extracts motion by delaying one input signal and multiplying it with a non-delayed signal to detect movement across the visual scene (highlighted in yellow). Panel (B) illustrates the Elementary Small Target Motion Detector (ESTMD) [14], which builds upon the delay-and-correlate principle (see green dotted box). It captures the motion of a tiny target by correlating the bright leading edge (highlighted in red) and the dark trailing edge (highlighted in blue), with one signal delayed and the other not. In contrast, panel (C) presents the proposed dual-dynamics-and-correlate mechanism, offering a novel approach to detecting tiny target motion independent of the delay parameter τ within the delay-and-correlate mechanism shown in (A) and (B). The orientation of the detected target is determined using the proposed strategy illustrated in panel (E). Next, panel (D) showcases the conventional approach for orientation determination, employing individual directional encoding and position-exclusive decoding [15]. Panel (E) introduces our proposed collaborative directional encoding-decoding strategy, in which encoding is shared globally across spatial locations, enabling spatially integrated decoding. This collaborative strategy greatly minimizes encoding computational demands compared to the isolated strategy shown in (D).

1) *EMD mechanism*: Elementary motion detector (EMD), also known as the "HR detector" or "HR correlator," was first introduced by Hassenstein and Reichardt in 1956. Their model relied on the multiplication of a center arm signal and the delayed one from the peripheral arm, resulting in motion and direction selectivity when the signals coincided in readout neurons [9].

A decade later, Barlow and Levick proposed a new model based on studies of the rabbit retina, in which they divided the central arm signal by the delayed peripheral arm. This model became known as the "BL detector" [10]. In 2016, Haag *et al.* proposed a detector combining the HR and BL detectors, grounded in biological studies that suggested such nonlinear interactions require at least three inputs [16]. The following year, Arenz *et al.* critically evaluated the three-input model and its input elements [11].

As these mechanisms all rely on coincident signals to detect motion and estimate direction, they belong to the delay-and-correlate mechanism. Given an input $I(\vec{z}, t)$ and assuming the output is $O(\vec{z}, t)$, where \vec{z} represents plane space coordinates and t denotes time, those mechanisms can be mathematically described as follows:

Hassenstein-Reichardt(HR) detector (preferred-direction

(PD) enhancement) [9]:

$$O(\vec{z}, t) = I(\vec{z}', t - \tau) * I(\vec{z}, t). \quad (1)$$

Barlow-Levick(BL) detector (null-direction (ND) suppression) [10]:

$$O(\vec{z}, t) = \frac{I(\vec{z}, t)}{I(\vec{z}', t - \tau)} \quad (2)$$

HR/BL detector (PD enhancement with ND suppression) [11], [16]:

$$O(\vec{z}, t) = \frac{I(\vec{z}', t - \tau_1) * I(\vec{z}, t)}{I(\vec{z}', t - \tau_2)} \quad (3)$$

2) *Delay-and-correlate based motion detector*: Based on the efficient and lightweight delay-and-correlate mechanism, numerous computational models have been developed over the past few decades. Some studies have combined two or more EMDs to compute visual odometry for navigation [17], simulate fly fixation behavior [18], and estimate angular velocity in the bee brain [19].

Leveraging the advantages of ON/OFF pathways [20], several studies have utilized the 2-Quadrant (2-Q) EMD to detect light (ON-EMD) and dark (OFF-EMD) edge translation [21].

Joesch *et al.* [22] conducted an in-depth study of the 2-Q detector, challenging the 4-Q detector proposed by [9]. Additionally, Clark *et al.* [23] presented a 6-Quadrant (6-Q) detector to explore turning behavior in *Drosophila*.

Furthermore, some studies applied the delay-and-correlate mechanism in mimicking lobula plate tangential cells (LPTCs) to estimate background motion direction in cluttered environments [24], and modeled LPLC2 to shape ultra-selectivity for approaching objects located at the center of the receptive field [25]. Other works focused on extracting ON/OFF moving edges [26] and proposed a "time-to-travel" method [27].

In conclusion, the delay-and-correlate mechanism provides a foundational framework for understanding how physiological visual systems recolonize motion patterns through efficient and lightweight networks, especially within low-level pathways. However, it does not perform well in modeling STMDs, a topic that will be discussed in the following sections.

B. Small target motion detectors

Bio-inspired Small Target Motion Detector (STMD) models draw inspiration from the behavior of specialized neurons in the insect visual system, aiming to replicate this visual pathway as a lightweight visual detector [28]. These neurons are highly responsive to tiny moving targets within a visual angle of 1° – 3° while exhibiting minimal responsiveness to larger targets exceeding 10° [5]–[8]. Current STMD models are all derived from the delay-and-correlate mechanism, which detects tiny target motion by correlating two or more coincident input signals from ON (brightness increase) and OFF (brightness decrease) pathways [20].

The backbone of STMD models with a four-layer structure (see Fig. 4 (A)) includes ESTMD [14] and DSTMD [15], where only the latter is directional sensitive. The ESTMD model utilizes ON/OFF signals at the identical spatial location to track tiny target motion by adjusting the delay between ON-OFF pathways, calculated as $\frac{l}{v}$, where l is the target size along motion path and v is target velocity [14]. To discriminate motion direction, Wang *et al.* (2020) proposed a directionally-selective small target motion detector (DSTMD) that correlates ON/OFF inputs from two spatial locations with different delays [15]. Notably, two cascaded models, ESTMD-EMD and EMD-ESTMD, also can identify the motion direction of tiny targets [29].

Over the past decade, efforts have been made to enhance the functionality of STMD-based models and improve their detection performance. Notable advancements include the STMD+ model [30], time-delay feedback neural networks (FeedbackSTMD) [13], attention and prediction guided visual systems (ApgSTMD) [31], modelling with feedback loop (\mathcal{F} STMD) [32], STMD with Spatio-Temporal Feedback [33], and Haar-based (hSTMD) [34]. Additionally, Xu *et al.* remodeled the lamina in STMD models using a fractional-difference operator to reduce reliance on high-frequency input [1]. Moreover, Chen *et al.* prove that the dynamics of translational visual motion are consistently maintained in STMD computational models, supporting this area with mathematical foundations [35]. Furthermore, in hardware implementation,

Zahra *et al.* [36], [37] demonstrate the effectiveness and robustness of the bio-inspired algorithm for STMD in real-world scenarios.

Next, we will explain the main mechanisms in ESTMD [14] and DSTMD [15] using mathematical formats. The locating process utilizes only one spatial location input with ON and OFF pathways. However, identifying direction requires the combination of at least two spatial location inputs.

1) *Elementary small target motion detector (ESTMD)*: The core operators of ESTMD [14] include a temporal derivation in Lamina with ON-OFF pathways, a signal delay in Medulla, and the correlate mechanism in Lobula.

Differentiation:

$$L(\vec{z}, t) = \frac{dI(\vec{z}, t)}{dt} \quad (4)$$

ON-OFF pathway:

$$L_{ON}(\vec{z}, t) = [L(\vec{z}, t)]^+; L_{OFF}(\vec{z}, t) = [L(\vec{z}, t)]^- \quad (5)$$

Delay-and-correlation between identical-spatial ON-OFF pathways:

$$O(\vec{z}, t) = L_{ON}(\vec{z}, t) * L_{OFF}(\vec{z}, t - \tau) \quad (6)$$

2) *Directionally-sensitive small target motion detector (DSTMD)*: The DSTMD [15] model shares the same Lamina and Medulla layers as the ESTMD model, and its Lobula correlation can be described as follows.

Delay-and-correlation within multi-spatial ON-OFF pathways:

$$O(\vec{z}, t, \theta) = L_{ON}(\vec{z}, t) * L_{OFF}(\vec{z}', t - \tau_3) * [L_{ON}(\vec{z}, t - \tau_1) + L_{OFF}(\vec{z}', t - \tau)] \quad (7)$$

where

$$\vec{z}' = \vec{z} + \alpha * (\cos \theta, \sin \theta). \quad (8)$$

Based on the above backbones of STMD models, we found that neither ESTMD nor DSTMD backbones nor other STMD models need the time parameter τ to make sure the multi-input of ON and OFF pathways coincident in the output layer. As a result, the model only performs well when τ is closed to $\frac{l}{v}$. In real-world scenarios, it is challenging to establish an optimal parameter that can effectively accommodate the varying sizes and velocities of tiny targets. Therefore, proposing a new correlation model for STMD real-world implementation is necessary.

III. METHODS AND FORMULATIONS

In this section, we first introduce the dual-dynamics-and-correlate mechanism, followed by the collaborative directional encoding-decoding strategy. Next, we illustrate the proposed directional backbone STMDNet and an improved version of STMDNet-F.

A. Dual-dynamics-and-correlate mechanism

To capture the tiny target motion cues of multi-velocity-to-length radii, we adopt dynamics potentials incorporating ipsilateral excitatory and contralateral inhibition junctions for the ON-OFF pathway in the medulla, resulting in dual dynamics. These two dynamic potentials are correlated for locating and will be reused in the next section for the proposed collaborative directional encoding-decoding strategy, as shown in Fig. 2 (C) and (E).

(Technical details here will be uploaded in a later version)

B. Collaborative directional encoding-decoding strategy

The proposed collaborative directional encoding-decoding strategy is divided into two steps, shared encoding and spatially integrated decoding, as shown in Fig. 2 (E). Specifically, we adopt the shared encoding to get local directional-field coding (LDFC) via a point-to-point indicated division for dual dynamics, where motion is marked by a transition from low to high gradients. Finally, motion directions are calculated via a weighted sum of surrounding LDFC with the weight of unit direction vectors, but we use spatially integrated decoding rather than position-exclusive decoding (see Fig. 2 (D)) in [15].

(Technical details here will be uploaded in a later version)

Notably, in each location, the direction weight is obtained by directly reading its neighboring LDFC values in spatially-integrated decoding, boosting the Information utilization efficiency, as shown in see Fig. 2 (E). As a result, the collaborative directional encoding-decoding strategy greatly minimizes encoding computational loads compared to the isolated directional encoding-decoding strategy combined with delay-and-correlate mechanism (see Fig. 2 (D)).

Moreover, we demonstrate the advantages of the proposed collaborative directional encoding-decoding strategy in Fig. 3, highlighting its robustness, accuracy, and efficiency. As shown in panel (A), the framework exhibits robustness by relying solely on information from the current target, specifically the front and rear motion edges (green hollow circles). The delay-and-correlate mechanism (indicated by the pink arrows) calculates correlations between a current motion edge and a previous one outside the current target (represented by solid pink circles). This method introduces background interference because it requires searching for the prior motion edge in multiple directions.

Panel (B) shows the accuracy of the proposed model in orienting a tiny moving target along a curved path. The motion trajectory of the target is depicted in purple, with the current ground truth direction indicated by a magenta arrow. We use green and pink arrows to represent the orientation indicated by the proposed strategy and the delay-and-correlate mechanism, respectively. The result illustrates that the proposed model closely aligns with the ground truth, demonstrating superior accuracy by effectively utilizing current motion edges. In contrast, the delay-and-correlate mechanism exhibits huge orientating errors due to its dependence on spatial information

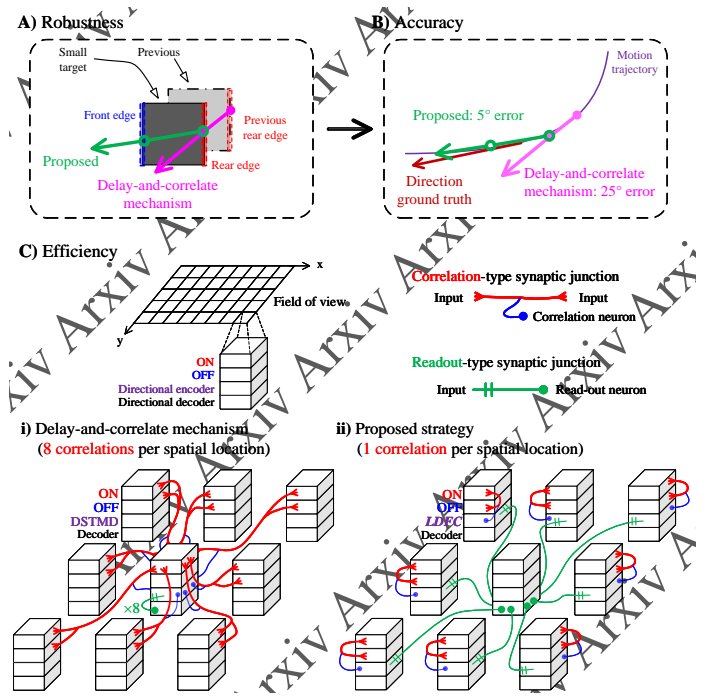


Fig. 3. Robustness, accuracy, and efficiency of the proposed collaborative directional encoding-decoding strategy compared with delay-and-correlate mechanism combined with isolated directional encoding-decoding strategy. (A) illustrates the robustness of the proposed framework (green arrows) with only leveraging front and rear motion edges (green hollow circle). In comparison, the delay-and-correlate mechanism (pink arrows) calculates correlations between a current motion edge and a previous motion edge outside the current target (solid pink circle), making it susceptible to interference from background motion. (B) shows the high directional accuracy of the proposed framework. (C) highlights the efficiency of the proposed strategy over the delay-and-correlate type isolated directional encoding-decoding strategy. For simplicity, we illustrate a central location and eight surrounding locations, along with how directional information can be calculated, where the neuron names are indicated in the upper left corner. In the proposed mechanism, direction information can be directly readout from LDFCs without additional computation. Consequently, the proposed mechanism requires only one correlation per spatial location for LDFCs, while the delay-and-correlate mechanism necessitates eight correlations between ON and OFF signals at each spatial location.

beyond the target's edge, which reflects the previous motion cue.

Panel (C) highlights the computational efficiency of the two models by comparing their correlation requirements. A central location and its eight surrounding locations are depicted, along with the method for calculating directional information, with neuron names indicated in the upper-left corner. Sub-panel (i) shows the delay-and-correlate mechanism with isolated directional encoding-decoding strategy in Fig. 2 (D), which requires **eight correlations** per spatial location, resulting in a dense network of connections between "ON" and "OFF" channels. In contrast, the proposed model needs **only one correlation** per spatial location under the global mean sense by sharing the LDFC, significantly simplifying the connection complexity, as shown in sub-panel (ii).

C. New backbone for STMD-based model

Building on the above dual-dynamic-and-correlate mechanism and collaborative directional encoding-decoding strategy,

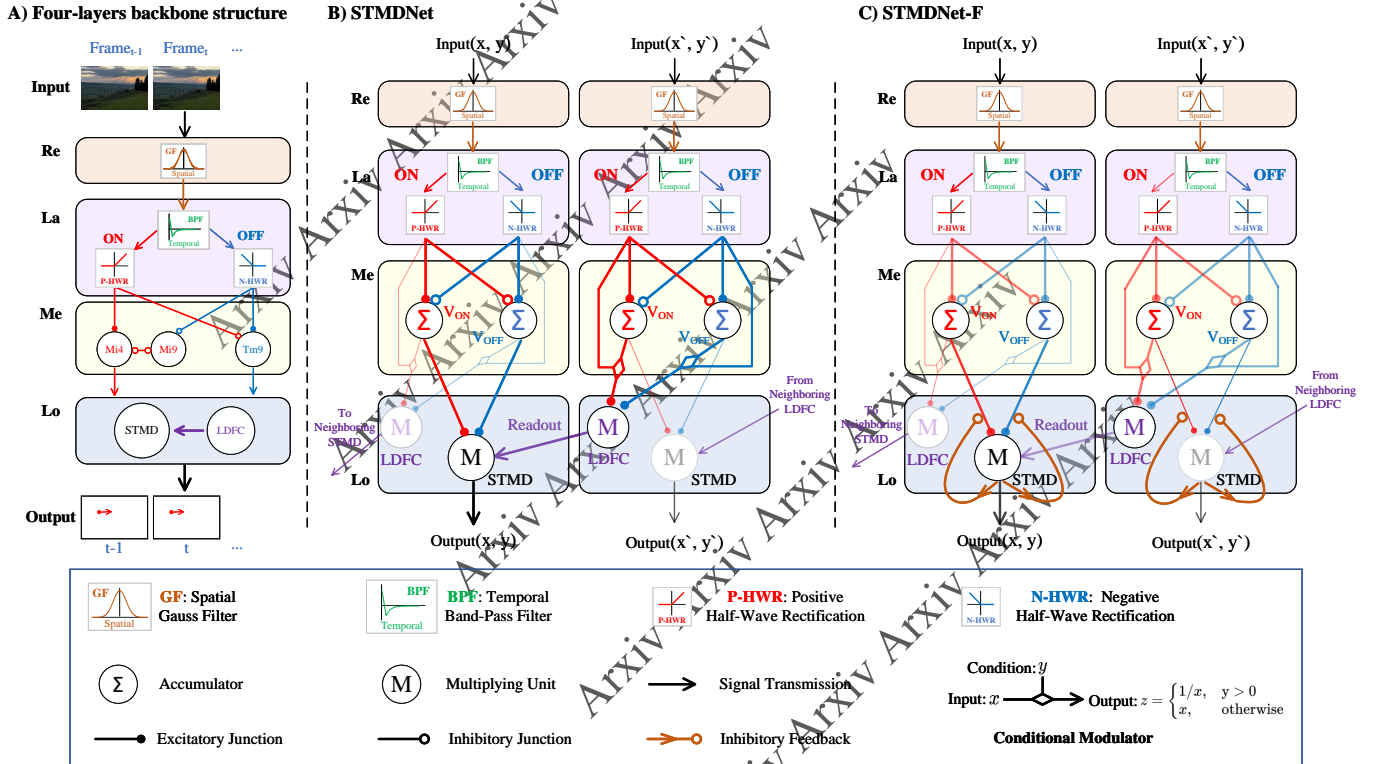


Fig. 4. Diagram of the proposed backbone. (A) shows the four-layer structure of the STMD-based model. The input image stream is successively smoothed by the retina and then separated into brightness increases (ON signals, red) and brightness decreases (OFF signals, blue). These signals are then processed parallelly by ON and OFF in Medulla, before being fused in the lobula. (B) and (C) illustrate pixel-level diagrams of the proposed lightweight directional backbone (STMDNet) and its improved version (STMDNet-F) with the feedback pathway proposed by [13]. The proposed backbone shares the dual dynamics for both the locating part (STMD) and the orientating part (LDFC), bringing its efficiency, where STMD identifies motion direction by read-outing the information by LDFC. (Abbreviations: Re: retina, La: lamina, Me: medulla, Lo: lobula.)

we propose a biologically plausible STMD network in this subsection, named STMDNet denoting a lightweight directional backbone. The backbone consists of four layers: the retina, lamina, medulla, and lobula, as shown in Fig. 4 (A) and (B). The input signal is received and filtered by retinal photoreceptors, differentiated into ON and OFF pathways in the lamina, and further processed in the medulla before reaching STMD in the lobula.

(Technical details here will be uploaded in a later version)

D. Improved version STMDNet-F

As shown in Fig. 4 (C), we integrate the existing feedback pathway from [13] into the proposed backbone, STMDNet, resulting in an enhanced version, STMDNet-F. The feedback pathway significantly suppresses background movement that is slower than the target. In STMDNet-F, we only modify the locating part in the lobula while the other parts remain the same as the STMDNet.

(Technical details here will be uploaded in a later version)

The experiments in Sect. IV show that STMDNet-F outperforms FeedbackSTMD [13] with a 24% improvement by simply replacing the backbone, demonstrating that the proposed

STMDNet serves as a more suitable backbone for current STMD models.

IV. EXPERIMENTAL RESULTS

In this section, we begin by outlining the experimental setup, which includes the datasets, comparison models, evaluation criteria, and implementation details. We then present results from synthetic datasets to validate the effectiveness of multi-velocity localization, direction identification, and implementation under low sampling frequencies. This also allows us to explore response curves and analyze relevant parameters. Following this, we discuss the results from our comparison experiments using real-world datasets. Finally, we provide some discussions.

A. Experimental setup

1) *Datasets:* This study employs two distinct datasets for evaluation: simulated datasets generated using VisionEgg [41] and real-world datasets referred to as RIST [42]. Both datasets feature dynamic backgrounds influenced by ego-motion, providing a challenging environment for model evaluation.

The simulated datasets consist of multiple videos with a resolution of 470×310 pixels. Each video depicts a synthetic target moving against a built-in panoramic background. These synthetic targets vary in luminance, velocity, size, and frame

TABLE I
REVIEW OF SEVERAL TINY TARGET MOTION RECOGNITION METHODS ACCORDING TO THEIR DESIGN AND OUTPUT

Method	Publication	Year	Model?	Component	Directional?	Time Per Frame
ESTMD [14]	Plos-One	2008	Model	STMD-based Backbone	N	17.83 ms
DSTMD [15]	T-Cybernetics	2020	Model	STMD-based Backbone	Y	54.31 ms
RPFC [4]	T-Cybernetics	2020	ANN	Random Projection Feature with Clustering	N	1184.89 ms
STMD+ [30]	T-NNLS	2020	Model	DSTMD [15] + Contrast Pathway [30]	Y	90.58 ms
FeedbackSTMD [13]	T-NNLS	2021	Model	ESMTD [14] + Feedback Pathway [13]	N	21.21 ms
ApgSTMD [31]	T-Cybernetics	2022	Model	STMDplus [30] + Apg Pathway [31]	Y	169.18 ms
\mathcal{F} STMD [32]	Front. Neurobot.	2023	Model	ESTMD [14] + Feedback Loop [32]	N	15.08 ms
Frac-STMD [1]	Neurocomputing	2023	Model	Frac-Lamina [1] + EMD mechanism [9]	N	5.44 ms
ZBS [3]	CVPR	2023	DNN	Unsupervised Zero-sort Deep Learning	N	342.03 ms (GPU)
STMDNet	Ours	-	Model	Frac-Lamina [1] + Proposed mechanisms	Y	11.43 ms
STMDNet-F	Ours	-	Model	STMDNet + Feedback Pathway [13]	Y	19.55 ms

rate, enabling a comprehensive assessment of the proposed model’s performance under diverse conditions.

The RIST datasets [42] comprises 19 videos totaling 29,900 frames, each with a resolution of 270×480 pixels and a frame rate of 240 Hz. The videos feature moving targets ranging in size from 3×3 to 10×10 pixels. These targets exhibit variable-speed motion against diverse, cluttered backgrounds such as skies, buildings, trees, grass, and shrubs, under both sunny and cloudy conditions. This variety provides a rich foundation for evaluating the model’s robustness and generalizability in real-world scenarios.

2) *Comparison model*: For comparison, we selected seven STMD models, ESTMD [14], DSTMD [15], Frac-STMD [1], STMD+ [30], ApgSTMD [31], FeedbackSTMD [13], and \mathcal{F} STMD [32], along with RPFC [4] and a advanced deep learning-based model, ZBS [3]. The details of these models are provided in Table I, with their inference speeds evaluated using the RIST dataset.

3) *Evaluation criteria*: In our evaluation, we assess detection quality using AUC, AP, and F1-score, while measuring computational efficiency with Time per Frame. The AUC, Area Under Curve of Recall-FPPI (false positive per image), measures the overall performance of the model in binary classification tasks, indicating its ability to distinguish between positive and negative classes. The AP (Average Precision) summarizes the precision-recall curve by calculating the weighted mean of precision at each threshold, offering insight into the model’s precision across different recall levels. The F1-score, defined as the harmonic mean of precision and recall, balances these two metrics to evaluate the model’s ability to accurately identify true positives while minimizing false positives and false negatives.

4) *Implementation Details*: All experiments presented in this paper were conducted using Python 3.9 and MATLAB R2024b on a personal laptop equipped with a 2.50 GHz Intel Core i5-12500 CPU and 16 GB of DDR5 memory. Notably, the deep learning-based method ZBS [3] is run on an NVIDIA GeForce RTX 3050 Laptop GPU with 4GB of GPU memory. The implementation of the STMD models was carried out using the open-source toolbox Small-Target-Motion-Detectors (STMD version 2.0) [43]. Additionally, the source code for the other methods are available at <https://github.com/MingshuoXu/STMDNet>.

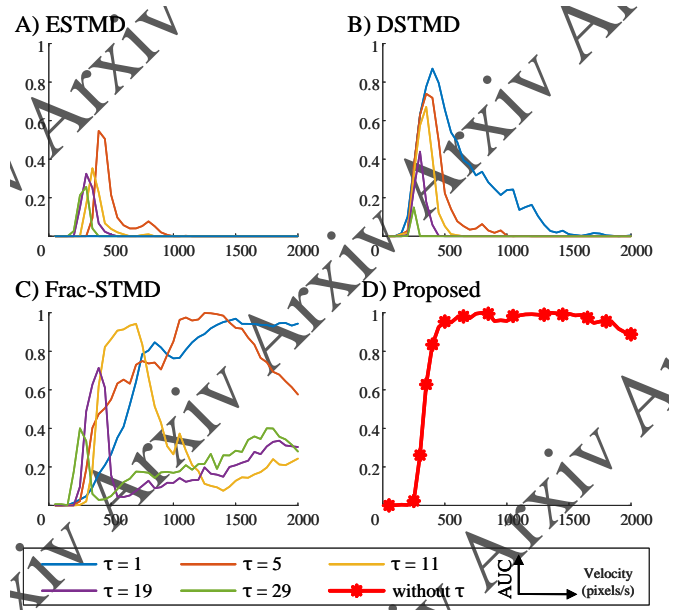


Fig. 5. Velocity-AUC curve. The optimal velocities for (A) ESTMD, (B) DSTMD, and (C) FracSTMD shift right as τ decreasing. In contrast, the proposed STMDNet, (D), demonstrates robust and stable performance across multiple velocities without tuning delay parameter τ .

[//github.com/MingshuoXu/STMDNet](https://github.com/MingshuoXu/STMDNet).

B. Results on synthetic datasets

In this subsection, we present results on synthetic datasets, including the effectiveness across multiple velocities and directions, as well as response curves and parameter analysis.

(Technical details here will be uploaded in a later version)

C. Comparison on real world datasets

In this subsection, we present a series of quantitative comparisons between the proposed STMDNet and STMDNet-F and other detectors on the RIST datasets [42].

(Technical details here will be uploaded in a later version)

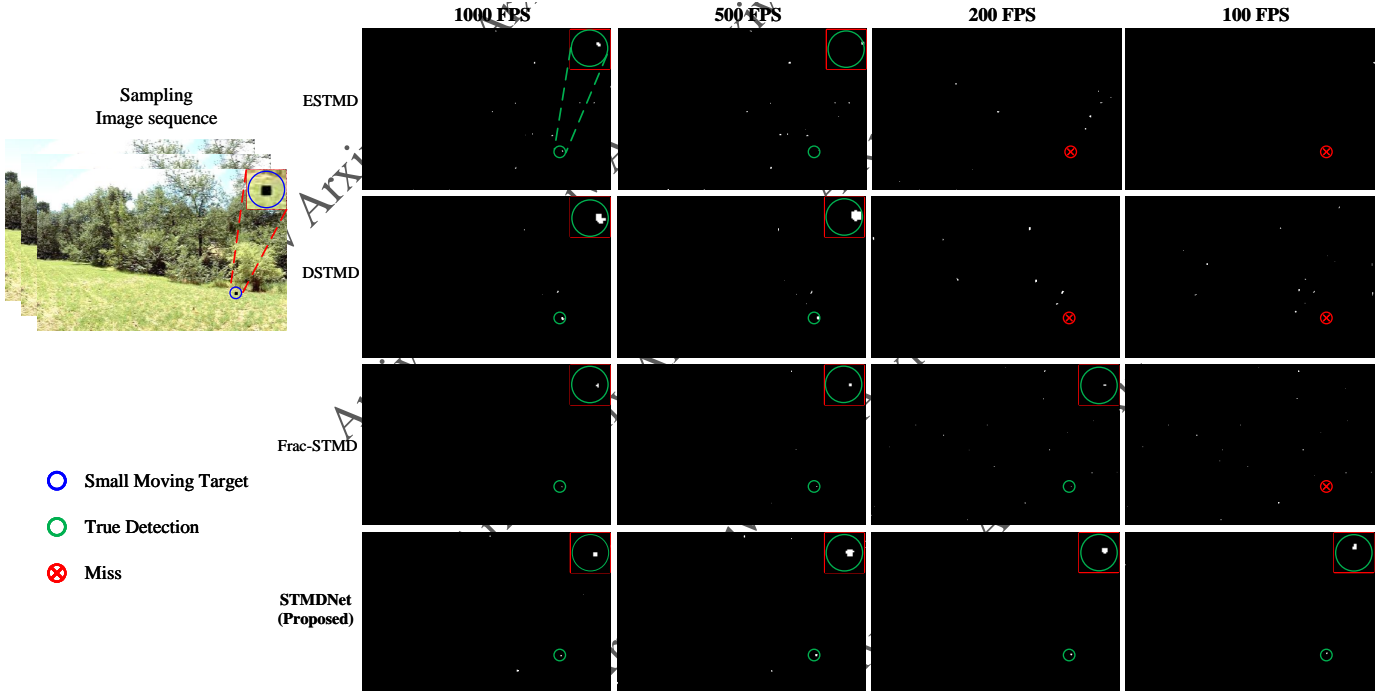


Fig. 6. Effectiveness across different sampling rates (1000 FPS, 500 FPS, 200 FPS, and 100 FPS). The leftmost column displays the input color image sequence, with the ground truth target marked in a blue circle and zoomed-in within the top right corner. The second to fifth columns present results from different FPS: 1000Hz, 500Hz, 200Hz, and 100Hz concerning ESTMD [14], DSTMD [15], and Frac-STMD [1], and the proposed model. In each sub-panel, correct detections are indicated by green circles, while misses are shown with red crosses. Zoomed-in views of these markings are provided in the top-right corner. The proposed model demonstrates robust detection across all sampling rates, maintaining consistent accuracy even at lower frame rates, whereas other models show increasing misses as the frame rate decreases.

TABLE II
RESULTS ON RIST [42] UNDER MULTI SAMPLING FREQUENCIES: HIGHER VALUES INDICATE BETTER DETECTION PERFORMANCE

Method	240Hz (Original)			120Hz (Down-sampling)			60Hz (Down-sampling)		
	mAUC(%)	mAP(%)	mF ₁ (%)	mAUC(%)	mAP(%)	mF ₁ (%)	mAUC(%)	mAP(%)	mF ₁ (%)
ESTMD [14]	20.47	6.52	8.25	8.03	1.60	2.13	2.01	0.47	0.58
DSTMD [15]	27.97	12.36	15.16	11.88	3.98	5.12	3.98	0.73	0.90
STMD+ [30]	35.42	17.86	21.54	19.68	8.71	10.84	7.23	2.04	2.73
FeedbackSTMD [13]	39.27	14.82	18.39	19.19	5.70	7.46	6.71	1.35	1.83
ApgSTMD [31]	25.86	6.03	7.13	13.46	1.72	2.14	6.26	0.98	1.28
\mathcal{F} STMD [32]	39.19	20.05	24.22	21.14	9.47	11.86	8.00	2.35	3.18
Frac-STMD [1]	38.41	15.52	19.25	35.62	13.79	17.22	30.12	10.77	13.77
RPFC [4]	-	19.12	12.96	-	4.38	5.87	-	1.07	2.09
ZBS [3]	-	23.51	22.83	-	21.58	21.37	-	21.69	21.81
STMDNet (Ours)	53.99	34.45	38.78	48.33	28.47	33.18	35.51	19.62	23.45
STMDNet-F (Ours)	63.70	39.29	43.84	57.39	32.62	37.72	49.03	25.29	30.31

D. Discussion

As demonstrated in the foregoing subsection, we verified the effectiveness of the proposed backbone in terms of locating and orientating and low sampling frequency implementation. Further conducted extensive comparative experiments on real-world datasets, the superior performance and efficiency of STMDNet and STMDNet-F confirm their suitability for real-time applications in dynamic environments, especially those requiring rapid and accurate tiny target motion recognition.

Furthermore, while we demonstrate STMDNet boosting Feedback STMD [13] by about 24% (STMDNet-F), it is crucial to consider its compatibility with other existing mech-

anisms such as feedback loops [32], contrast pathways [30], and attention and predictive mechanisms [31]. Many current models incorporate parameters that are inherently tied to predefined velocity assumptions. One important direction for future research is exploring how these mechanisms can be adapted or re-engineered to align with the new backbone, which operates without needing prior velocity-related parameters. Investigating the integration of these mechanisms with the proposed backbone could lead to more flexible and robust models capable of handling a wider range of dynamic environments, further advancing the field of motion detection.

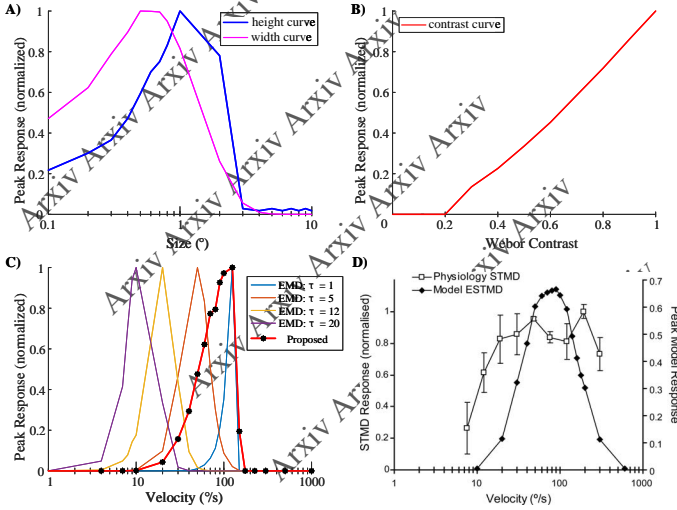


Fig. 7. Normalized tuning curves of the proposed model, presented relative to (A) target size, (B) contrast, and (C) target velocity, where panel (C) compares velocity tuning with the EMD mechanism (FracSTMD) across multiple delay parameters τ . Panel (D) summarizes the response characteristics of physiological STMDs, adapted from [14].

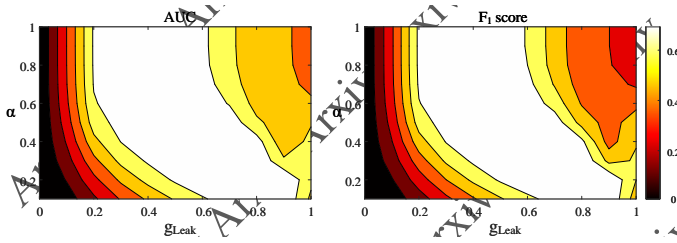


Fig. 8. Parameter analysis using contour maps with respect to the contour maps of AUC and F1-score.

V. CONCLUSION

In this work, we present a novel framework, STMDNet, which incorporates a dual-dynamics-and-correlation mechanism and pioneers the first collaborative directional encoding-decoding strategy. These innovations replace the traditional delay-and-correlate mechanisms and isolated directional encoding-decoding strategy for locating and orienting, improving the detecting performance, especially under low sampling frequency scenarios. By decoupling the small target motion detection with a fixed size-to-velocity ratio, STMDNet achieves a new SOTA baseline, offering several significant advantages to this research field, as outlined below.

First, with the dual-dynamics-and-correlate mechanism, target localization is independent of the tuning parameter, delay time (τ). In a word, we rid the STMD models of single size-to-velocity ratio target detection, which is better suited for real-world implementation of tiny targets with varying sizes and velocities.

Second, we propose the first collaborative directional encoding-decoding strategy, which provides a new approach for direction identification, enhancing accuracy, robustness, and efficiency. The new strategy adopts the globally shared encoding calculated by only one computational load in each spatial location and spatially integrated decoding to achieve

the motion direction. It improves computational efficiency compared to the traditional method, which utilizes individual encoding with eight computational loads at each location. Moreover, it improves accuracy and robustness in detecting deflecting motion by focusing on motion edge information while reducing interference from the background.

Third, effective utilization of motion cues enhances functionality across various sampling frequencies. Particularly, the STMDNet improves the performance at 60 Hz, breaking through the bottleneck of the existing model using high sampling frequencies, like 240 Hz, to capture essential motion cues. As a result, the proposed framework broadens the model's applicability, addressing the challenge of the substantial computational power required to capture and process high-sampling-frequency videos.

Additionally, the STMDNet is biological plausibility, delivering exceptionally fast processing speeds with 87 FPS on a single thread within a CPU. Compared to the huge computational demands of deep learning methods, the proposed framework is agile enough to be implemented in insect-sized or other lightweight robots. Further, evaluations of STMDNet-F demonstrate that, the proposed framework makes STMD hold the lead in model-based models and come from behind to win with data-driven deep learning models.

Last but not least, as the delay-and-correlate mechanisms have been widely used in various motion detection models over the past decades (see Sect. II-A2), our proposed framework, by offering a novel and more efficient alternative, has the potential to inspire a wide range of researchers and practitioners in the field. Thus, we hope our work will encourage further exploration and advancements in motion detection technologies, breathing new life into the model-based methodology.

CREDIT AUTHORSHIP CONTRIBUTION STATEMENT

Mingshuo Xu: Methodology, Software, Writing - Original Draft, Visualization. **Hao Luan:** Methodology, Validation, Writing - Review & Editing. **Zhou Daniel Hao:** Conceptualization, Writing - Review & Editing. **Jigen Peng:** Formal analysis, Funding acquisition. **Shigang Yue:** Supervision, Writing - Review, Funding acquisition.

DECLARATION OF COMPETING INTEREST

The authors declare that they have no known competing financial interests or personal relationships that could have appeared to influence the work reported in this paper.

ACKNOWLEDGMENT

This research was supported in part by the European Union's Horizon 2020 Research and Innovation Program through the Marie Skłodowska-Curie Grant under Agreement 778602 ULTRACEPT, and in part by the National Natural Science Foundation of China under Grant 12031003.

REFERENCES

- [1] M. Xu, H. Wang, H. Chen, H. Li, and J. Peng, "A fractional-order visual neural model for small target motion detection," *Neurocomputing*, vol. 550, p. 126459, 2023.
- [2] A. Alfano, L. Maiano, L. Papa, and I. Amerini, "Estimating optical flow: A comprehensive review of the state of the art," *Computer Vision and Image Understanding*, p. 104160, 2024.
- [3] Y. An, X. Zhao, T. Yu, H. Guo, C. Zhao, M. Tang, and J. Wang, "Zbs: Zero-shot background subtraction via instance-level background modeling and foreground selection," in *Proceedings of the IEEE/CVF Conference on Computer Vision and Pattern Recognition*, 2023, pp. 6355–6364.
- [4] J. Wang, G. Zhang, K. Zhang, Y. Zhao, Q. Wang, and X. Li, "Detection of small aerial object using random projection feature with region clustering," *IEEE Transactions on Cybernetics*, vol. 52, no. 5, pp. 3957–3970, 2020.
- [5] K. Nordström and D. C. O'Carroll, "Small object detection neurons in female hoverflies," *Proceedings of the Royal Society B: Biological Sciences*, vol. 273, no. 1591, pp. 1211–1216, 2006.
- [6] K. Nordström, P. D. Barnett, and D. C. O'Carroll, "Insect detection of small targets moving in visual clutter," *PLoS biology*, vol. 4, no. 3, p. e54, 2006.
- [7] P. D. Barnett, K. Nordström, and D. C. O'carroll, "Retinotopic organization of small-field-target-detecting neurons in the insect visual system," *Current Biology*, vol. 17, no. 7, pp. 569–578, 2007.
- [8] K. Nordström, "Neural specializations for small target detection in insects," *Current opinion in neurobiology*, vol. 22, no. 2, pp. 272–278, 2012.
- [9] B. Hassenstein and W. Reichardt, "Systemtheoretische analyse der zeit-, reihenfolgen- und vorzeichenbewertung bei der bewegungsperzeption des rüsselkäfers chlorophanus," *Zeitschrift für Naturforschung B*, vol. 11, no. 9-10, pp. 513–524, 1956. [Online]. Available: <https://doi.org/10.1515/znb-1956-9-1004>
- [10] H. Barlow and W. R. Levick, "The mechanism of directionally selective units in rabbit's retina." *The Journal of physiology*, vol. 178, no. 3, p. 477, 1965.
- [11] A. Arenz, M. S. Drews, F. G. Richter, G. Ammer, and A. Borst, "The temporal tuning of the drosophila motion detectors is determined by the dynamics of their input elements," *Current Biology*, vol. 27, no. 7, pp. 929–944, 2017.
- [12] M. Frye, "Elementary motion detectors," *Current Biology*, vol. 25, no. 6, pp. R215–R217, 2015.
- [13] H. Wang, H. Wang, J. Zhao, C. Hu, J. Peng, and S. Yue, "A time-delay feedback neural network for discriminating small, fast-moving targets in complex dynamic environments," *IEEE Transactions on Neural Networks and Learning Systems*, 2021.
- [14] S. D. Wiederman, P. A. Shoemaker, and D. C. O'Carroll, "A model for the detection of moving targets in visual clutter inspired by insect physiology," *PLoS ONE*, vol. 3, no. 7, pp. e2784–, 2008.
- [15] H. Wang, J. Peng, and S. Yue, "A directionally selective small target motion detecting visual neural network in cluttered backgrounds," *IEEE Transactions on Cybernetics*, vol. 50, no. 4, pp. 1541–1555, 2020.
- [16] J. Haag, A. Arenz, E. Serbe, F. Gabbiani, and A. Borst, "Complementary mechanisms create direction selectivity in the fly," *Elife*, vol. 5, p. e17421, 2016.
- [17] F. Iida, "Biologically inspired visual odometer for navigation of a flying robot," *Robotics and autonomous systems*, vol. 44, no. 3-4, pp. 201–208, 2003.
- [18] A. Bahl, G. Ammer, T. Schilling, and A. Borst, "Object tracking in motion-blind flies," *Nature neuroscience*, vol. 16, no. 6, pp. 730–738, 2013.
- [19] A. J. Cope, C. Sabo, K. Gurney, E. Vasilaki, and J. A. Marshall, "A model for an angular velocity-tuned motion detector accounting for deviations in the corridor-centering response of the bee," *PLoS computational biology*, vol. 12, no. 5, p. e1004887, 2016.
- [20] Q. Fu, "Motion perception based on on/off channels: a survey," *Neural Networks*, vol. 165, pp. 1–18, 2023.
- [21] N. Franceschini, A. Riehle, and A. Le Nestour, "Directionally selective motion detection by insect neurons," in *Facets of vision*. Springer, 1989, pp. 360–390.
- [22] M. Joesch, F. Weber, H. Eichner, and A. Borst, "Functional specialization of parallel motion detection circuits in the fly," *Journal of Neuroscience*, vol. 33, no. 3, pp. 902–905, 2013.
- [23] D. A. Clark, L. Bursztyn, M. A. Horowitz, M. J. Schnitzer, and T. R. Clandinin, "Defining the computational structure of the motion detector in drosophila," *Neuron*, vol. 70, no. 6, pp. 1165–1177, 2011.
- [24] H. Wang, J. Peng, and S. Yue, "An improved lptc neural model for background motion direction estimation," in *2017 Joint IEEE International Conference on Development and Learning and Epigenetic Robotics (ICDL-EpiRob)*. IEEE, 2017, pp. 47–52.
- [25] M. Hua, Q. Fu, J. Peng, S. Yue, and H. Luan, "Shaping the ultra-selectivity of a looming detection neural network from non-linear correlation of radial motion," in *2022 International Joint Conference on Neural Networks (IJCNN)*. IEEE, 2022, pp. 1–8.
- [26] S. Yue and Q. Fu, "Modeling direction selective visual neural network with on and off pathways for extracting motion cues from cluttered background," in *2017 International Joint Conference on Neural Networks (IJCNN)*. IEEE, 2017, pp. 831–838.
- [27] N. Franceschini, J.-M. Pichon, and C. Blanes, "From insect vision to robot vision," *Philosophical Transactions of The Royal Society Of London. Series B: Biological Sciences*, vol. 337, no. 1281, pp. 283–294, 1992.
- [28] Q. Fu, H. Wang, C. Hu, and S. Yue, "Towards computational models and applications of insect visual systems for motion perception: A review," *Artificial life*, vol. 25, no. 3, pp. 263–311, 2019.
- [29] S. Wiedermann and D. C. O'Carroll, "Biologically inspired feature detection using cascaded correlations of off and on channels," *Journal of Artificial Intelligence and Soft Computing Research*, vol. 3, 2013.
- [30] H. Wang, J. Peng, X. Zheng, and S. Yue, "A robust visual system for small target motion detection against cluttered moving backgrounds," *IEEE Transactions on Neural Networks and Learning Systems*, vol. 31, no. 3, pp. 839–853, 2020.
- [31] H. Wang, J. Zhao, H. Wang, C. Hu, J. Peng, and S. Yue, "Attention and prediction-guided motion detection for low-contrast small moving targets," *IEEE Transactions on Cybernetics*, 2022.
- [32] J. Ling, H. Wang, M. Xu, H. Chen, H. Li, and J. Peng, "Mathematical study of neural feedback roles in small target motion detection," *Frontiers in Neurorobotics*, vol. 16, p. 984430, 2022.
- [33] H. Wang, Z. Zhong, F. Lei, J. Peng, and S. Yue, "Bio-inspired small target motion detection with spatio-temporal feedback in natural scenes," *IEEE Transactions on Image Processing*, 2023.
- [34] H. Chen, X. Sun, C. Hu, H. Wang, and J. Peng, "Unveiling the power of haar frequency domain: Advancing small target motion detection in dim light," *Applied Soft Computing*, vol. 167, p. 112281, 2024.
- [35] H. Chen, B. Fan, H. Li, and J. Peng, "Rigid propagation of visual motion in the insect's neural system," *Neural Networks*, vol. 181, p. 106874, 2025.
- [36] Z. M. Bagheri, B. S. Cazzolato, S. Grainger, D. C. O'Carroll, and S. D. Wiederman, "An autonomous robot inspired by insect neurophysiology pursues moving features in natural environments," *Journal of neural engineering*, vol. 14, no. 4, p. 046030, 2017.
- [37] Z. M. Bagheri, S. D. Wiederman, B. S. Cazzolato, S. Grainger, and D. C. O'Carroll, "Performance of an insect-inspired target tracker in natural conditions," *Bioinspiration & biomimetics*, vol. 12, no. 2, p. 025006, 2017.
- [38] E. J. Warrant, "Matched filtering and the ecology of vision in insects," *The ecology of animal senses: matched filters for economical sensing*, pp. 143–167, 2016.
- [39] Y. E. Fisher, J. C. Leong, K. Sporar, M. D. Ketkar, D. M. Gohl, T. R. Clandinin, and M. Silies, "A class of visual neurons with wide-field properties is required for local motion detection," *Current Biology*, vol. 25, no. 24, pp. 3178–3189, 2015.
- [40] B. De Vries and J. Principe, "A theory for neural networks with time delays," *Advances in neural information processing systems*, vol. 3, 1990.
- [41] A. D. Straw, "Vision egg: an open-source library for realtime visual stimulus generation," *Frontiers in neuroinformatics*, p. 4, 2008.
- [42] H. Wang, "Rist data set." 2019, accessed: 2022-01-11. [Online]. Available: <https://sites.google.com/view/hongxinwang-personalsite/download>
- [43] M. Xu, "Small-target-motion-detectors, version 2," 2024, accessed: 2024-09-26. [Online]. Available: <https://github.com/MingshuoXu/Small-Target-Motion-Detectors>